Journal of the European Ceramic Society **15** (1995) 81–88
© 1995 Elsevier Science Limited
Printed in Great Britain. All rights reserved
0955-2219/95/$9.50

Chlorine and Oxygen Inhibition Effects in the Deposition of SiC-based Ceramics from the Si–C–H–Cl System

D. Lespiaux,[a] F. Langlais,[a] R. Naslain,[a] S. Schamm[b] & J. Sevely[b]

[a] Laboratoire des Composites Thermostructuraux, UMR 47, CNRS, SEP, UB1 Domaine Universitaire 3 allée de la Boëtie, 33600-Pessac, France
[b] Centre d'Elaboration de Matériaux et d'Etudes Structurales, Laboratoire d'Optique Electronique, UPR 8011, CNRS, BP 4347, 31055 Toulouse Cedex, France

(Received 19 November 1993; accepted 13 June 1994)

Abstract

The inhibitory role of HCl and oxygen in the chemical vapour deposition of SiC-based ceramics from the Si–C–H–Cl system, is pointed out in terms of nucleation and growth process on the basis of experimental and theoretical approaches. The addition of HCl to methyltrichlorosilane MTS–H_2 gaseous precursors (i) decreases the nucleation and growth rate, (ii) induces a transition from a diffusion to a reaction rate control of the deposition process, (iii) improves the smoothness of the films surface, (iv) results in a transition from anisotropic films with columnar microstructure and Si, C and O concentration gradients to nanocrystallized materials with quite constant Si, C and O contents. These behaviours are tentatively explained by assessments of the gas phase supersaturation and calculations of the chemisorbed layer composition. The occurrence of oxygen within the nanocrystallized films is then related to the growth inhibition effect and the presence of silicon excess shown by EELS analyses.

1 Introduction

Chemical vapour deposition (CVD) is a suitable technique to prepare silicon carbide films of high quality. Owing to its good thermal, mechanical and chemical properties, SiC is used as a ceramic matrix in fibre-reinforced ceramic–ceramic composites elaborated by chemical vapour infiltration (CVI), a technique which derives directly from CVD.[1,2]

Most of SiC-depositions involve the Si–C–H–Cl chemical system. The organometallic compound CH_3SiCl_3 (MTS) is often used as precursor partly for its ability to be decomposed at moderate temperatures (which usually favours the CVI process), and partly for economical reasons.[3–6]

A model was proposed recently to simulate and optimize the homogeneity and the rate of the infiltration in a single straight cylindrical pore.[7] This model, when applied to the CVI of SiC in the MTS–H_2 system,[8] pointed out the fundamental role of HCl in the control of the quality of the infiltration. Hydrogen chloride is successively produced by (i) the homogeneous decomposition of MTS precursor and (ii) the heterogeneous reaction of SiC deposition from carbon and silicon intermediate species.[9] The infiltration gradient along the pore is related to the HCl concentration which is found, at the pore centre, to be very similar to those of source species at the entrance.[8]

The first purpose of the present paper is to assess the influence of HCl content in the precursor gas mixture on: (i) the nucleation and growth processes and (ii) the physico-chemical nature of the deposits performed on an amorphous SiO_2 substrate. The effects resulting from a HCl excess will be discussed on the basis of supersaturation estimates and chemisorption calculations.

Under well-defined conditions, the MTS–H_2 precursor provides nanocrystalline SiC films with silicon excess and a small amount of oxygen.[10] The second purpose of this article is to correlate the silicon excess (and oxygen content) with the growth rate, through chemisorption data previously calculated.[11] Finally, a structural model will be proposed for these nanocrystalline SiC-based ceramic films, built on EELS analyses including both valence and inner-shell electron excitations.

Journal of the European Ceramic Society 0955-2219/95/$9.50 © 1995 Elsevier Science Limited, England. Printed in Great Britain

2 Experimental

The various procedures and equipments which have been used for both the nucleation/growth experiments and the physico-chemical characterization of the films, have been described in detail in Ref. 10.

The deposition experiments were performed in a vertical hot-wall CVD reactor working under reduced pressure. The initial composition of the MTS–HCl–H_2 gas precursor is given by α and δ defined as follow:

$$\alpha = \frac{P_{H_2}}{P_{MTS}} = \frac{Q_{H_2}}{Q_{MTS}} \quad (1)$$

$$\delta = \frac{P_{HCl}}{P_{MTS}} = \frac{Q_{HCl}}{Q_{MTS}} \quad (2)$$

where P_i, and Q_i are the initial partial pressures and flow rates of species i. A microbalance was used to detect the transient and steady-state stages in the deposition process and to determine the various growth rates. The substrates were amorphous silica layers obtained by oxidizing silicon wafers. To investigate the nucleation process, very short experiments were carried out, followed by (i) SEM observations of the resulting nuclei and (ii) determination of the nucleation characteristics such as the saturation nucleus density N_S, the saturation nucleus size ϕ_S and the nucleation rate I.[10]

After a first microstructural approach by SEM and X-ray diffraction, transmission electron microscopy (TEM) (bright-field and dark-field observations and selected area electron diffraction) combined with local (60 or 30 nm diameter probe sizes) electron energy loss spectroscopy analysis (EELS) were used for a description of the SiC-based films at a nanometric scale. The local chemical and structural organization of the films was investigated by using core excitations (Si-L, C-K and O-K edges) and volume plasmon characteristic signals.

3 Influence of HCl Content on the Deposition Process of SiC-based Ceramics

3.1 Nucleation process

When the initial MTS–H_2 mixture contains HCl, the initial stages of the deposition are highly modified. As shown in Fig. 1, for T = 1100°C, P = 3 kPa and α = 30, the SiO_2 surface is not totally covered by SiC-based deposit after an exposure of 2600 s to a MTS–H_2–HCl mixture (with δ = 0·5), while the saturation is almost performed after 45 s of exposure to MTS–H_2 mixture (with δ = 0). An important decrease of the nucleation rate from $2{\cdot}5 \times 10^{12}$ to 3×10^8 is readily achieved by adding 50% HCl to the MTS source, but a further increase of HCl initial concentration does not modify the nucleation rate any longer. Moreover, when δ = 0·5, nuclei are not adjacent but form aggregates from only a few sites. This result can be correlated with an inhibition effect of HCl on a SiO_2 surface.

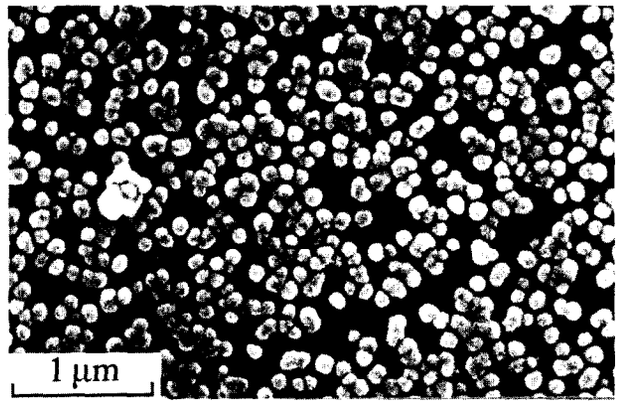

(a)

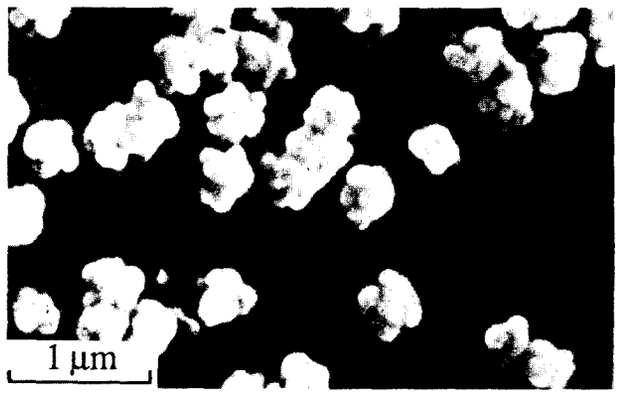

(b)

Fig. 1. SEM pictures of nucleus density observed on SiO_2 substrates for T = 1100°C, α = 30, P = 3 kPa and (a) δ = 0 and after an exposure time of 45 s, and (b) δ = 0·5 after an exposure time of 2600 s.

3.2 Growth kinetics

When the steady state is reached, the deposition rate can be deduced from the slope of the mass–time curves. The variations of this rate as a function of HCl partial pressure (ratio varying from 0·1 to 1) are plotted in Fig. 2 for α = 10, P = 3 kPa and two temperatures (1000 and 1100°C). The growth rate is observed to decrease when δ increases above 0·2. This result confirms the inhibition effect of HCl, previously mentioned for the nucleation process.

To identify the kinetic regime of the deposition, the growth rate was studied as a function of the temperature and the total flow rate, for two initial compositions of the gas phase ((i) α = 10 and δ = 0, (ii) α = 10 and δ = 1), the total pressure being 3 kPa, the temperature ranging from 1000 to 1125°C and the total flow rate from 200 to 550 sccm (Figs 3 and 4). When δ = 0, the deposition rate does not depend significantly on the temperature (Fig. 3) and it increases continuously with the total flow rate (Fig. 4). This behaviour is typical for a kinetic

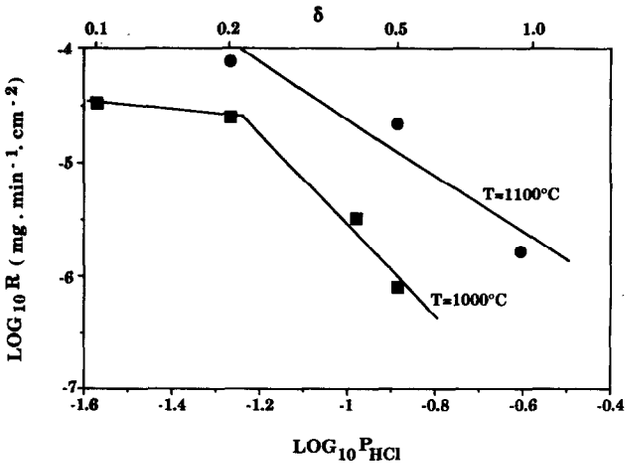

Fig. 2. Variations of the deposition rate R versus HCl partial pressure PHCl and δ ratio for α = 10, P = 3 kPa and ■, T = 1000°C; ●, T = 1100°C.

process controlled by mass transport, e.g. by diffusion through a boundary layer. When δ = 1, the growth rate decreases exponentially with the reciprocal temperature and does not depend on the total flow rate. This second behaviour, which corresponds to a kinetic control by the surface reactions, can be explained by a decrease of the heterogeneous reaction rate due to the inhibition effect of added HCl. As a consequence, the addition of HCl to the gaseous precursor results in a transition from a diffusion rate control to a reaction rate control of the deposition of SiC-based ceramics. This type of transition was already evidenced for BN deposition in the B–N–H–F system: it was induced by variations of the temperature, the total pressure and also the initial composition of the gas phase.[12,13]

3.3 Physico-chemical characteristics of the deposits

As demonstrated in a related paper, the change in the kinetic regime of SiC-based ceramic deposition has a great influence on the microstructure of the films.[10] When a diffusion-controlled kinetic process is changed to a reaction-controlled one (by

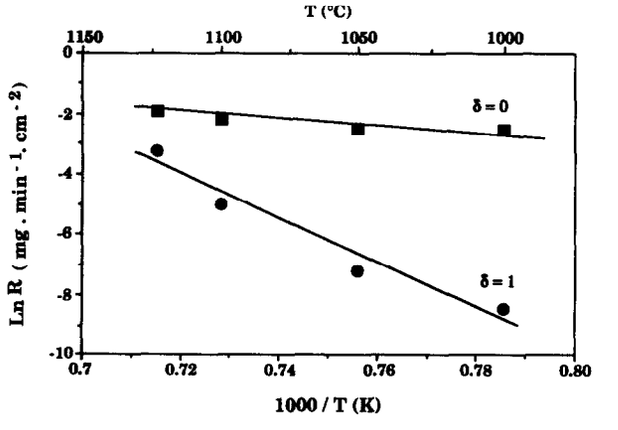

Fig. 3. Variations of the logarithm of the deposition rate R versus reciprocal temperature for α = 10, P = 3 kPa, Q = 400 sccm and ■, δ = 0, ●, δ = 1.

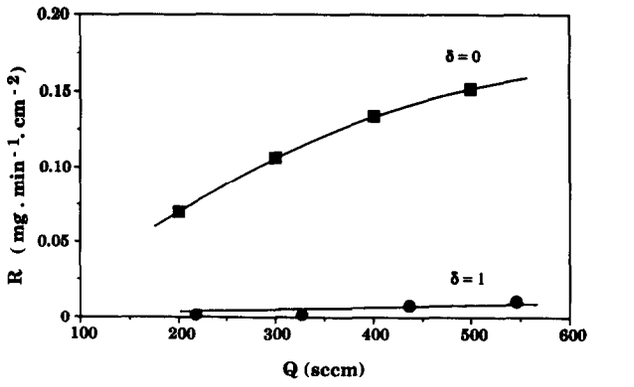

Fig. 4. Variations of the deposition rate R versus total flow rate Q for T = 1100°C, α = 10, P = 3 kPa and ■, δ = 0; ●, δ = 1.

varying temperature and/or total pressure), a transition occurs from a crystallized film with columnar crystals to a nanocrystalline deposit. Thus, a detailed experimental investigation was performed in order to show whether the kinetic transition presently induced by adding HCl to the initial gas mixture results or not in similar microstructural changes.

3.3.1 Morphology and microstructure

The surface morphology of the films deposited for 1100°C, α = 10 and P = 3 kPa is influenced by the addition of HCl to the MTS–H_2 mixture (Fig. 5).

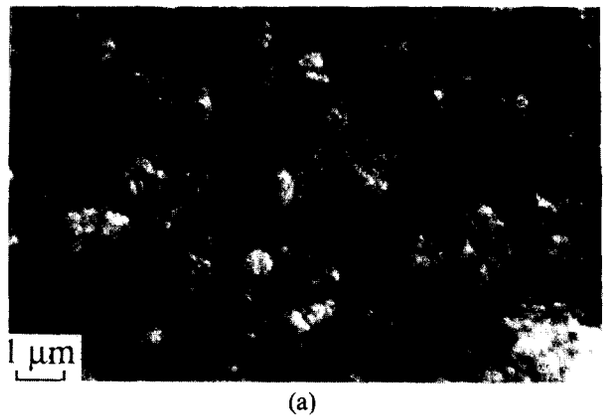

(a)

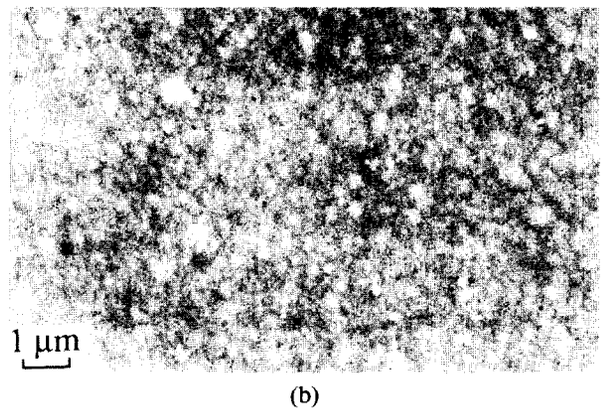

(b)

Fig. 5. SEM pictures showing the surface morphology of SiC-based deposits obtained for T = 1100°C, α = 10, P = 3 kPa and (a) δ = 0; (b) δ = 0·5.

Table 1. X-Ray (CuK_α) analyses of SiC-based deposits on SiO_2 substrates for T = 1100°C, α = 10, P = 3 kPa and various δ ratios

δ	0	0·2	0·5	*References from ASTM tables*
Crystallite size (nm)	14	11	7	
I^a (111) (% a.u)	100	100	100	100
I^a (220) (% a.u)	1·5	2	8	63

[a] $I_{(111)}$ and $I_{(220)}$ represent respectively the intensities of the (111) and (220) diffraction lines.

When δ is raised from 0 to 0·5, i.e. when the kinetics become controlled by the surface reactions, the roughness of the surface is decreased, a feature which is consistent with previous results reported in Ref. 10 for SiC and Ref. 12 for BN deposition.

X-Ray diffraction analyses of the films deposited under the same T, P, α conditions for δ = 0, 0·2 and 0·5 show again the preferred growth of silicon carbide along the ⟨111⟩ crystallographic direction perpendicular to the substrate surface (Table 1). Nevertheless, the increase of HCl content in the gas phase seems to weaken this textural effect. The Scherrer formula, applied to the (111) X-ray diffraction line of the diffraction patterns without taking into account the internal stress effect, leads to crystallite apparent sizes decreasing with increasing δ values.

The nanostructure of the films prepared under the same T, P, α values and without HCl in the precursor changes when moving from the interface with the substrate to the external surface, as supported by TEM observations. Figure 6 shows dark-field images obtained by selecting with the objective aperture a part of the first electron diffraction ring (mainly SiC (111)). In the observation, close to the substrate, a nanocrystalline material is shown with isotropic grains of about 5 nm in size (Fig. 6(a)). From 500 nm away from the substrate, an anisotropy is observed, giving rise to a slightly columnar microstructure (Fig. 6(b)). Conversely, when δ = 0·5, no microstructure variation is observed through the thickness of the film (Fig. 7): the whole deposited material being nanocrystalline and rather homogeneous.

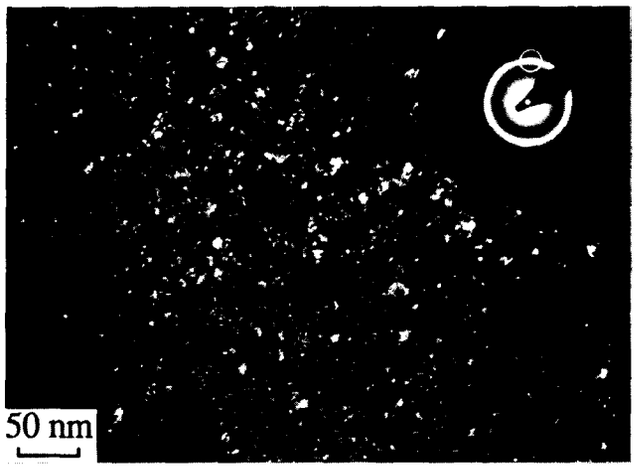

(a)

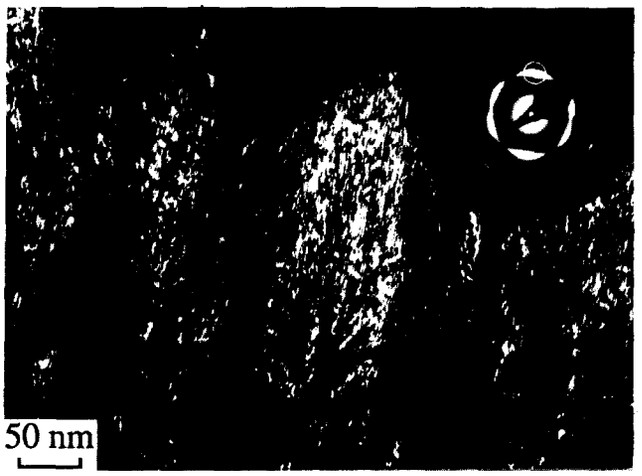

(b)

Fig. 6. Dark-field images and SAD patterns (inserts) of a SiC-based deposit on a SiO_2 substrate for T = 1100°C, α = 10 and P = 3 kPa, (a) near the substrate, (b) at 1 μm from the substrate.

3.3.2 Chemical composition

The relative concentrations of Si, C and O have been assessed by local EELS analyses which were carried out as a function of d, the distance from the substrate/deposit interface, for the samples prepared under the following conditions: T = 1100°C, α = 10, P = 3 kPa and δ = 0 or 0·5.

For the MTS–H_2 precursor (δ = 0), Si and C are present near the deposit/substrate interface in proportions respectively above and below the values corresponding to stoichiometric SiC (Fig. 8(a)). Conversely, from d = 400 nm, the silicon to

Fig. 7. Dark-field image and SAD pattern (insert) of a SiC-based deposit on a SiO_2 substrate T = 1100°C, α = 10, P = 3 kPa and δ = 0·5 at 1 μm from the substrate.

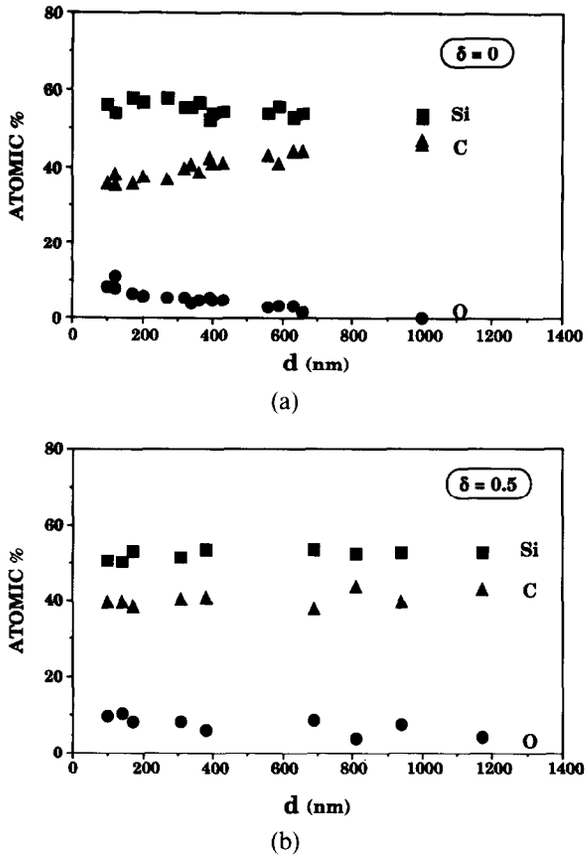

Fig. 8. Variations of Si, C and O contents with the distance d measured between the analysed area and the substrate/deposit interface, in SiC-based films obtained for T = 1100°C, α = 10, P = 3 kPa and (a) δ = 0 and (b) δ = 0·5.

carbon ratio moves towards the stoichiometric ratio. In addition a small amount of oxygen occurs in the deposit close to the substrate and decreases to zero through the thickness of the film.

Conversely, when HCl is added to the initial MTS–H_2 mixture (for δ = 0·5), the chemical composition of the film is almost constant (Fig. 8(b)), which is in accordance with the rather homogeneous nanostructure of the material. Nevertheless, a slight decrease of the oxygen content is observed from the substrate/deposit interface to the external surface of the film.

3.4 Theoretical approach: supersaturation and chemisorption

3.4.1 Assessment of gas phase supersaturation

For T = 1100°C, P = 3 kPa and α = 10, a transition from a diffusion rate control to a reaction rate control of the deposition process is induced by adding HCl to the initial MTS–H_2 mixture. Consequently, when δ is very small (δ < 0·2), the local supersaturation (which represents the departure from heterogeneous equilibrium) close to the substrate, is very low: due to the concentration gradients occurring through the boundary layer, the local gas phase composition is almost given by the heterogeneous equilibrium. Nevertheless, this low supersaturation value cannot be easily calculated under such conditions.

Conversely, when δ is increased beyond 0·2, i.e. under conditions of kinetic regime controlled by surface reactions, the gas phase becomes highly supersaturated near the substrate surface and the calculation of the supersaturation is then possible. It is based (i) on the assumption of rapid homogeneous reactions and (ii) on any heterogeneous reaction giving rise to pure SiC deposition, e.g.:

$$CH_4 + SiCl_2 \rightarrow SiC_{(S)} + H_2 + 2HCl \qquad (3)$$

As detailed in a previous study,[10] the theoretical supersaturation γ can be written as:

$$\gamma = \frac{P_{CH_4} P_{SiCl_2}}{P_{H_2} P_{HCl}^2} \cdot K_P(T) - 1 \qquad (4)$$

where $K_P(T)$ is the equilibrium constant corresponding to the reaction (3) and P_{CH_4}, P_{SiCl_2}, P_{H_2} and P_{HCl} are the partial pressures close to the solid surface calculated under the assumption of the homogeneous equilibrium. γ values were calculated for δ varying from 0·2 to 1 and for various conditions of temperature and pressure. As shown in Fig. 9, in spite of a slight decrease, calculated γ values remain very high ($\gamma > 10^4$) for the investigated range of conditions.

3.4.2 Calculation of the chemisorbed layer composition

On the basis of a previously described approach of the Langmuir chemisorption on amorphous SiO_2 or β-SiC substrates,[11] the composition of the adsorbed layer in the CVD of SiC from the Si–C–H–Cl system was calculated for various HCl contents in the precursor.

Figure 10 shows the variations of coverages θ_i on a SiO_2 surface as a function of δ ratio for the conditions used in the nucleation experiments, i.e. for T = 1100°C, P = 3 kPa and α = 30. A highly

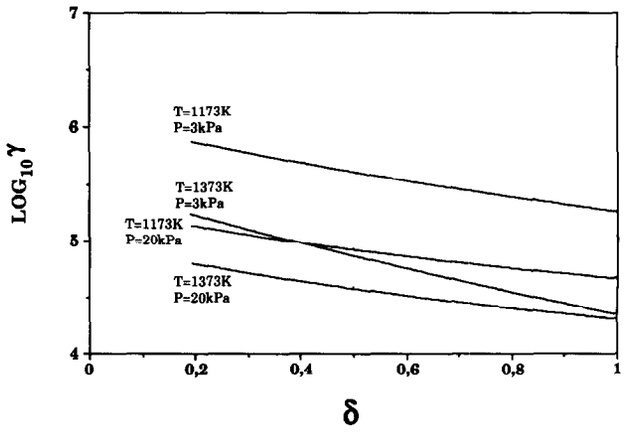

Fig. 9. Variations of the calculated supersaturation γ versus δ ratio ($[HCl]_{in}/[MTS]_{in}$) for various temperature and pressure conditions.

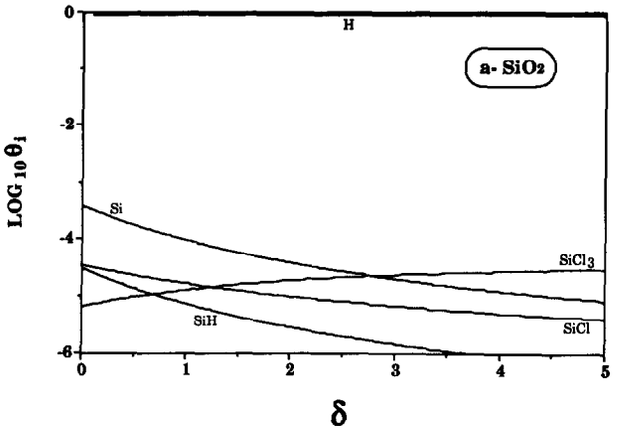

Fig. 10. Coverages of an oxygen plane of amorphous SiO_2 substrate versus δ ratio for T = 1100°C, α = 30 and P = 3 kPa.

dominant coverage is found for H radical over the whole δ range. The only source species coverages (i.e. the silicon containing species), are decreased by raising δ ratio, except for $SiCl_3$. Due to this decrease of silicon species, the addition of HCl to the gaseous precursor enhances the inhibition of the nucleation on a SiO_2 surface.

In Fig. 11, the coverages on a C(111) and a Si(111) plane of β-SiC are represented versus δ for T = 1100°C, P = 3 kPa and α = 30. For the C plane, the dominant adsorbed species are H and to a less extent C_2H_2 and $SiCl_3$ whose coverages are not influenced by δ. An increase of δ results only in the increase of Cl coverage which remains very low. For the Si plane, Cl and C_2H_2 are the main chemisorbed species. Cl coverage increases and the one of C_2H_2 decreases as δ rises. Here again, an inhibition effect of HCl, particularly on the formation of C on a Si(111) plane, is demonstrated by the chemisorption approach.

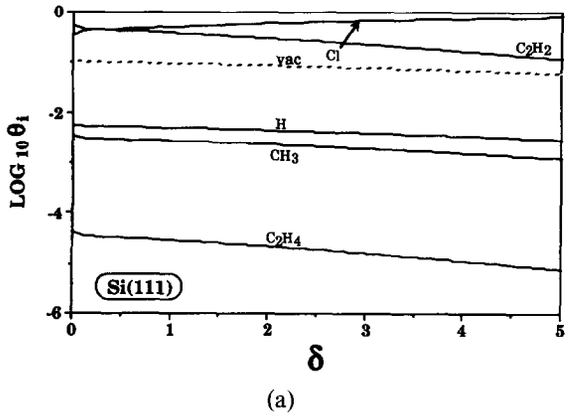

(a)

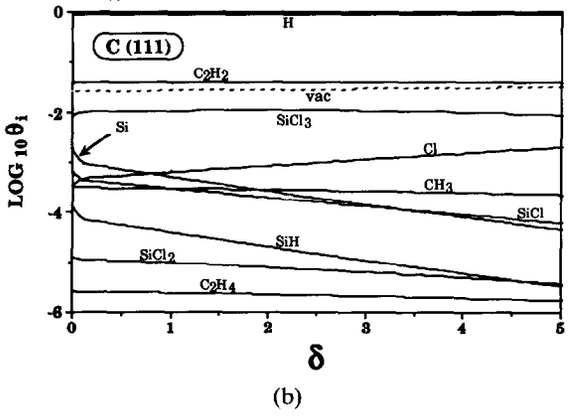

(b)

Fig. 11. Coverages of (a) a Si (111) plane of β-SiC and (b) a C (111) plane of β-SiC versus δ ratio for T = 1100°C K, α = 30 and P = 3 kPa.

3.5 Discussion

The present experimental and theoretical approach of the SiC-based ceramic deposition permits a correlation stated in a previous study between (i) the supersaturation of the gas phase close to the deposition surface, (ii) the crystallization state and (iii) the surface morphology of the deposit to be confirmed. A high increase of the local supersaturation, presently induced by the addition of HCl to the MTS–H_2 mixture, results in a transition from a deposit with a columnar microstructure and a rough surface to a rather smooth and nanocrystallized film.

The inhibitory effect of HCl is also pointed out in the present study. The nucleation process on amorphous SiO_2 surface is particularly inhibited by HCl. This effect is partly explained by a chemisorption of source species on SiO_2 unfavoured by HCl. The selectivity of the nucleation with respect to the nature of the substrate, reported in a previous paper,[11] is highly increased by introducing HCl in the initial gaseous mixture. A continuous renucleation regime is favoured on silicon carbide rather than on SiO_2, as shown in Fig. 1.

The growth process of silicon carbide itself is highly inhibited by the HCl enrichment of the precursor, a feature which confirms the assumptions proposed in previous investigations of the deposition[14] or infiltration mechanisms for the MTS–H_2

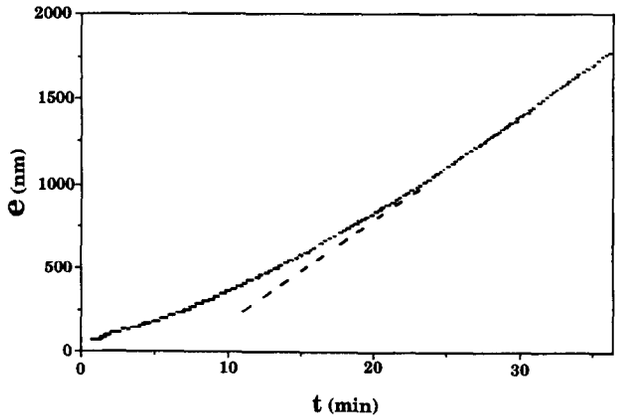

Fig. 12. Mass–time curve recorded during the deposit of a SiC-based film for T = 900°C, α = 3 and P = 3 kPa on a SiO_2 substrate.

system.[8,9] This inhibition can be explained partly by a higher coverage of Cl species on Si(111) planes of β-SiC. On the other hand, one of the main surface reaction assumed to lead to silicon formation from $SiCl_x$ intermediate, $1 \leq x \leq 3$, is probably rate-limited by the corresponding reaction:

$$SiCl_x^* + x/2\ H_2 \rightleftharpoons Si + xHCl + * \qquad (5)$$

where $SiCl_x^*$ represents the adsorbed form of $SiCl_x$ and * a free surface site. Equation (5) shows that an increase of HCl content in the gas phase can highly inhibit the growth process by favouring the reverse reaction.

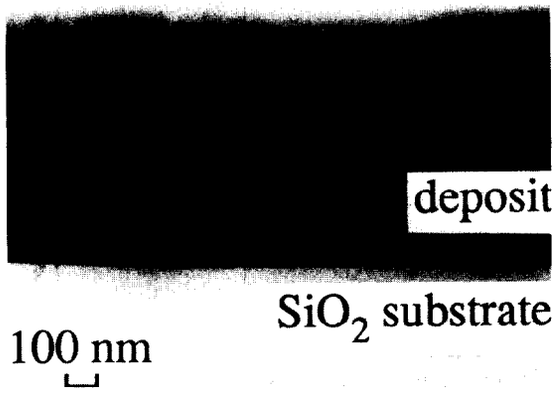

(a)

(b)

Fig. 13. (a) Bright-field image and (b) SAD pattern of a SiC-based deposit on a SiO_2 substrate or T = 900°C, α = 3 and P = 3 kPa.

4 Influence of Oxygen on the CVD Kinetic Process and Related Characteristics of SiC-based Ceramics

4.1 Growth rate

In a previous work, transient stages were reported for the mass–time curves recorded under conditions of high supersaturation, i.e. when the kinetic process is controlled by the surface reactions.[10] For T = 900°C, α = 3 and P = 3 kPa, a relatively long time (of about 25 mn) is needed to reach the steady state (Fig. 12). During the transient stage, the deposition rate is increasing continuously with time up to a value of about 5 μm h^{-1}.

4.2 Structural and chemical analysis by TEM and EELS

In order to explain this kinetic behaviour, a nano-characterization of the ceramic films prepared under the present conditions was carried out from a chemical and structural point of view. The TEM bright-field image in Fig. 13(a) shows that the deposit is nanocrystallized with an about 1·5 nm mean crystal size (Fig. 13(b)). Interreticular distances calculated from the diameter of the rings do not correspond to those of cubic β-SiC silicon carbide. This is related to a study of the relative concentrations of silicon and carbon, by using core excitation signals. These elements are present in proportions above and below the values corresponding to SiC respectively (Fig. 14). In addition, a small amount of oxygen is present in the deposit, which decreases with d to a few atomic percents. All these element concentrations change slowly but monotonically with thickness.

The corresponding valence energy loss study has been carried out. A single plasmon profile has been found for each analysed zone of the deposit, whose energy falls between the energies of Si and SiC plasmons (16·7 and 22·5 eV respectively)

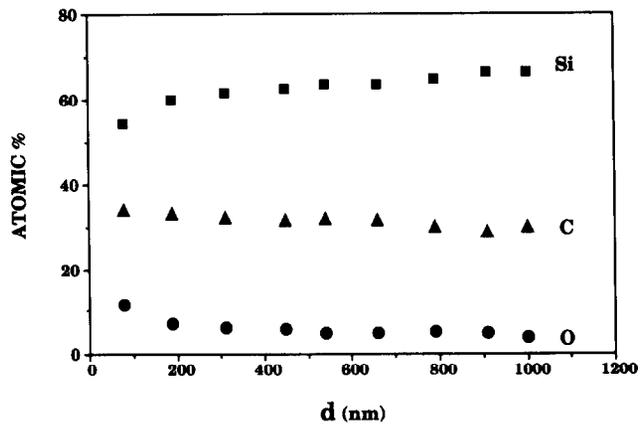

Fig. 14. Variations of Si, C and O contents with the distance d measured between the analysed area and the substrate/deposit interface, in a SiC-based film obtained at T = 900°C, α = 3, P = 3 kPa.

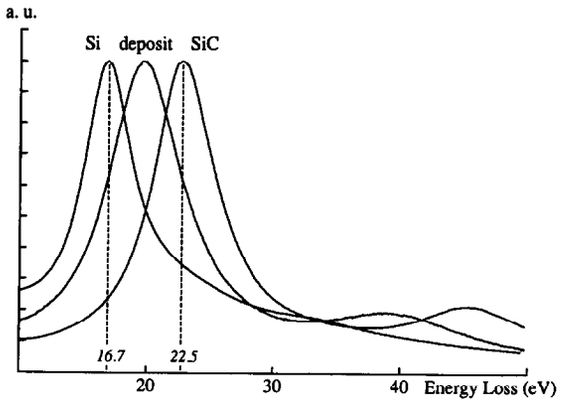

Fig. 15. Plasmon profiles of a SiC-based deposit (T = 900°C, α = 3, P = 3 kPa) and of Si and SiC reference materials.

(Fig. 15). It is also observed that this energy decreases progressively from 20·1 to 19·6 eV with d varying from 200 to 1000 nm in relation with the increase of the excess of silicon.

4.3 Discussion

The oxygen profile within the film could be correlated to the important transient stage observed in the kinetic curve: the growth rate increases when the oxygen percentage decreases and both become constant when $d > 750$ nm. This result means that oxygen might act as an inhibitor for the deposition of silicon carbide. As reported in a previous paper, the chemisorption of intermediate source species is unfavoured when the SiC substrate is replaced by an amorphous SiO_2 substrate, owing to the preferred chemisorption of the inhibitor species H (the O–H bond being very strong).[11] It has also been shown that oxygen occurs in nanocrystalline rather in columnar films.[10] The very small crystals in the former are thought to trap rather easily residual oxygen of the reactor, which results in blocking the growth sites by chemisorption of H atoms.

The above results have been used to propose a distribution of the Si, C and O elements within the deposit.[15] From thermodynamic considerations, on the one hand,[16] X-ray diffraction and Raman spectroscopy microprobe experiments, on the other hand,[9] carbon is known to be present only in silicon carbide and free silicon to be very often codeposited with silicon carbide. From the nanocrystallized structure of the deposit and the single profile of the plasmon loss which are observed, the occurrence of SiC nanocrystals including Si excess is assumed.[15]

Acknowledgements

The authors wish to thank Dr C. Bernard (LTPCM, Grenoble) for his contribution to the thermodynamic calculations, R. Fourmeaux and P. Salles (CEMES-LOE, Toulouse) for their support in electron microscopy experiments. This work has been supported by Société Européenne de Propulsion and CNRS (via a grant given to D. L.). The authors are indebted to J. Rey, C. Robin-Brosse and S. Goujard from SEP for their assistance and valuable discussions.

References

1. Hirai, T. & Sasaki, M., In *Silicon Carbide Ceramics—1*, ed. S. Somiya & Y. Inomata. Elsevier Science Publishers, London, New York, 1991, p. 77.
2. Naslain, R., Langlais, F. & Fedou, R., In *Proc. 7th Eur. Conf. on CVD*, ed. M. Ducarroir, C. Bernard L. Vandelbulcke. 1989, p. C5–191.
3. Schlichting, J., *Powder Metall. Int.*, **12**(3) (1980) 141 and **12** (4)(1980). 196.
4. Fitzer, E. & Gadow, R., *Am. Ceram. Soc. Bull.*, **65** (1986) 326.
5. Giso, M. & Chun, J., *J. Vac. Sci. Technol. A.*, **6**(1) (1988) 5.
6. Minato, K. & Fukuda, K., *J. Mater. Sci.*, **23** (1988) 699.
7. Fedou, R., Langlais, F. & Naslain, R., *J. Mater. Synth. Process*, **1**(1) (1993) 43.
8. Fedou, R., Langlais, F. & Naslain, R., *J. Mater. Synth. Process*, **1**(2) (1993) 61.
9. Langlais, F. & Prebende, C. In *Proc. 11th Int. Conf. on CVD*, ed. K. E. Spear & G. W. Cullen. The Electrochemical Society, Pennington, 1990, p. 686.
10. Lespiaux, D., Langlais, F., Naslain, R., Schamm, S. & Sevely, J., submitted to *J. Mater. Sci.*
11. Lespiaux, D. & Langlais, F., submitted to *Thin Solid Films.*
12. Prouhet, S., Langlais, F., Guette, A., Naslain, R. & Rey, J., *Eur. J. Solid State Inorg. Chem.*, **30** (1993) 953–69.
13. Prouhet, S., Vignoles, G., Langlais, F., Guette, A. & Naslain, R., *Eur. J. Solid State Inorg. Chem.*, **30** (1993) 971–89.
14. Besmann, T., Sheldon, B. W. & Kaster, M. D., *J. Am. Ceram. Soc.*, **75**(10) (1992) 2899.
15. Schamm, S., Kihn, Y., Severly, J., Lespiaux, D. & Langlais, F., *Proc. 10th Europ. Congress on Electron Microscopy*, Vol. 1. Granada, Spain, ed. A. Rios, J. M. Arias, L. Megras-Megras & A. Lopez-Galindo, 7–11 September 1992, p. 277.
16. Christin, F., Naslain, R. & Bernard, C., In *Proc. 7th Int. Conf. on CVD.* ed. T. O. Sedgwick. 1979, p. 499.